Metrol. Meas. Syst., Vol. 24 (2017), No. 2, pp. 357–368.

PAN POLSKA AKADEMIA NAUK

METROLOGY AND MEASUREMENT SYSTEMS

Index 330930, ISSN 0860-8229

www.metrology.pg.gda.pl

M&MS

MODELLING OF INFLUENCE OF HYPERSONIC CONDITIONS ON GYROSCOPIC INERTIAL NAVIGATION SENSOR SUSPENSION

Igor Korobiichuk[1)], Volodimir Karachun[2)], Viktorij Mel'nick[2)], Maciej Kachniarz[3)]

1) Warsaw University of Technology, Faculty of Mechatronics, Św. A. Boboli 8, 02-525, Warsaw, Poland (✉ igor@mchtr.edu.pl, +48 22 234 8506)

2) National Technical University of Ukraine, Kyiv Polytechnic Institute, 37 Peremogy, Kyiv, Ukraine (karachun11@i.ua, bti@fbt.ntu-kpi.kiev.ua)

3) Industrial Research Institute for Automation and Measurements PIAP, Al. Jerozolimskie 202, 02-486 Warsaw, Poland (mkachniarz@piap.pl)

Abstract

The upcoming hypersonic technologies pose a difficult task for air navigation systems. The article presents a designed model of elastic interaction of penetrating acoustic radiation with flat isotropic suspension elements of an inertial navigation sensor in the operational conditions of hypersonic flight. It has been shown that the acoustic transparency effect in the form of a spatial-frequency resonance becomes possible with simultaneous manifestation of the wave coincidence condition in the acoustic field and equality of the natural oscillation frequency of a finite-size plate and a forced oscillation frequency of an infinite plate. The effect can lead to additional measurement errors of the navigation system. Using the model, the worst and best case suspension oscillation frequencies can be determined, which will help during the design of a navigation system.

Keywords: hypersonic technologies, gimbals, oscillation modes, acoustic transparency, navigation system.

1. Introduction

Today, ships are armed with 100–145 mm calibre automatic cannons which have not only limited range but also insufficient shooting accuracy in a modern combat. Therefore, the main range of possible targets is acquired by missiles, which are very expensive and, besides, have considerable dimensions. To solve this problem, the United States Navy plans by 2025 to supply a rail gun capable of destroying any targets with cheap projectiles and at long ranges. The electromagnetic rail gun is developed by BAE SYSTEMS and GENERAL ATOMICS (Fig. 1). The testing is scheduled to take place on board of the newest high-speed vessel JHSV Millinocket.

Moreover, the developers of railguns offer to equip also usual powder cannons with hypersonic projectiles, which would dramatically improve their ability to hit any targets, including airborne ones.

Rail guns can project at a speed of 5M at a distance of 400 km. According to the military forecasts, such guns can hit any target. According to the Department for Development of Marine Systems of NAVSEA NAVY, the rail gun features are planned to be partly implemented in traditional powder cannons. It means, that an HVR hypersonic projectile is planned to be developed in two major United States Navy calibres: 155 mm and 127 mm. Thus, a universal core would serve for two types of both powder cannon and rail gun. Naturally, when firing from a powder cannon, the HVR speed would be lower than when firing from a rail gun. The difference would be 3 M and 5 M, respectively. Nevertheless, the speed will be twice higher than while using gunpowder. An HVR projectile should become an alternative to expensive

Article history: received on Dec. 01, 2016; accepted on Jan. 14, 2017; available online on Jun. 30, 2017; DOI: 10.1515/mms-2017-0024.

anti-aircraft missiles and 155 mm LRLAP projectiles which cost $ 400,000 per unit for Zumwalt class destroyers.

Fig. 1. A hypersonic projectile of a rail gun can replace expensive missiles.

However, advantages that create new means of fire support give rise to a lot of air navigation problems. They consist in high temperatures, extreme vibration, shock N-wave and penetrating acoustic radiation. Diffuse sound fields would fundamentally change the dynamics of on-board equipment mechanical systems' features and affect the performance characteristics of avionic instruments in general, such as inertial navigation systems.

Two-stage gyroscopic instruments are widely used as sensitive elements of gyroscopically stabilized platforms and inertial navigation systems. Therefore, the requirement of high precision indications is crucial for accurate building of reference directions on mobile objects. This applies primarily to the *launch vehicles* (LV) and hypersonic aircraft, the propulsion systems of which create a high sound pressure (up to 180 dB) in a rather broad frequency range. This will also apply to hypersonic projectiles, since the existing solid-state and MEMS systems are not accurate and simultaneously robust enough for such applications.

The main feature of penetrating radiation impact is its spatial nature. On the one hand, traditional means of combating external perturbations are ineffective, and, on the other hand, there is a need of a fundamentally new approach to design diagrams, namely a change from lumped parameter systems to distributed parameter systems. Let us demonstrate how this is applied to gimbals' flat fragments.

The goal of the research is to evaluate the risk of manifestation of local resonance peculiarities in gimbals when using an aircraft.

In order to achieve the aim, the following tasks should be accomplished:

1. Building a design diagram of the studied phenomenon.
2. Choosing a method of building a mathematical model with which particularities of resonance type would have been obvious and visible for further analysis when studying the dynamics of gimbals in general, especially to evaluate additional errors of autonomous positioning.
3. Evaluating feasibility and effectiveness of studying the phenomena using two-fold trigonometric series by normal functions in the rectangular area.
4. Assessing, according to two mutually perpendicular directions, the degree of influence of the plate vibration mode on the fullness of sound energy transmission through a flat barrier.

2. Material and methods

2.1. Sound wave diffraction at cross elastic gyroscope suspension

Supports with elasticity friction are used mainly in systems having limited rotation angles. In practice, such supports do not create a friction torque (as the value of elasticity friction is very low), have low accuracy of fixing the axis direction, but operate satisfactorily under heavy vibration. Depending on a type of elastic element deformation, there are bending supports and torsion supports.

A simple ribbon hinge is a plate connecting the fixed element to the moving element. This hinge is used, for example, as a pendulum suspension. The elastic hinge consists of a lever, two resilient plates and a fixed base. Such a hinge is used for small rotation angles of the moving part (1 ... 2 degrees). The track formed by intersection of extensions of the middle planes of elastic plates is taken as the rotation centre.

Figure 2 shows a cross hinge for two-stage gyroscope suspension 3, which is mounted on plate 1. Plate 1 is fixed on base 4 with a support consisting of four elastic plates 2, intersecting at an angle of $\alpha = 60^{\circ}... 90^{\circ}$ and attached to base 4 and plate 1. The rotation angle of these hinges may reach 30°.

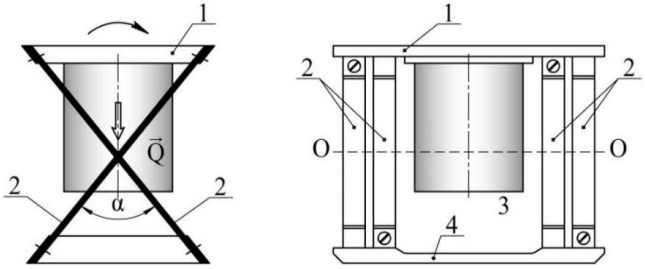

Fig. 2. A cross elastic hinge for a two-stage gyroscope suspension.

2.2. Cross elastic hinge. Mechanical model of interaction with acoustic radiation

We assume the cross angle $\alpha = \frac{\pi}{2}\ rad$ and analyse the structure of elastic interaction of acoustic radiation with a two-stage gyroscope suspension mounted on two cross hinges.

To better understand the nature of this phenomenon, we confine ourselves to consideration of the lowest forms of vibrations only. Moreover, for clarity, it is enough to study the waveform only in one direction.

We suppose that under the influence of an acoustic wave, elastic plates make a bending movement, taking only the first, lower form. Then, in the normal direction, one will receive movement r_1 and the other – r_2, which are represented as components of y_1, z_1 and y_2, z_2, and enable establishing that the notional pivot axis of the movable part of gyroscope will be moving along axis $Y - (y_1 + y_2)$ and axis $Z - (z_1 - z_2)$ (Fig. 3a). If these forms are manifested in phase at both cross hinges, the angular oscillations occur in respect to the conditional output axis O-O of the device (Fig. 3d). If they are manifested in antiphase, the gyroscope torsional oscillations occur in respect to Z axis (Fig. 3c).

If the first forms of plate flexural vibrations have a form shown in Fig. 3b, the form of gyroscope movements changes and upon the in-phase movement of the extreme points of O-O axis, the gyroscope makes the reciprocating movement along Z axis (Fig. 3e), while upon the antiphase movement the angular oscillations along the output axis occur.

Thus, the gyroscope suspension, upon acoustic loading, will produce straight fluctuations relative to axes, Y, Z and angular oscillations relative to axes X, Z. In this case a two-stage differentiating gyroscope has a bias, whereas a two-stage integrating gyroscope has a systematic drift. Furthermore, the device output signal also shows periodic components.

Leaving aside the issue of passing the acoustic wave through the proper gyroscope, a mechanical model of calculating the interaction of the overpressure wave P_{10} with the suspension can be represented in a form of two not interconnected elastic plates affected by a flat monochromatic wave (Fig. 4). Here, 1, 2, 3 are the falling, reflected and transmitted waves through the first plate, respectively, and 1′, 2′, 3′ – through the second plate.

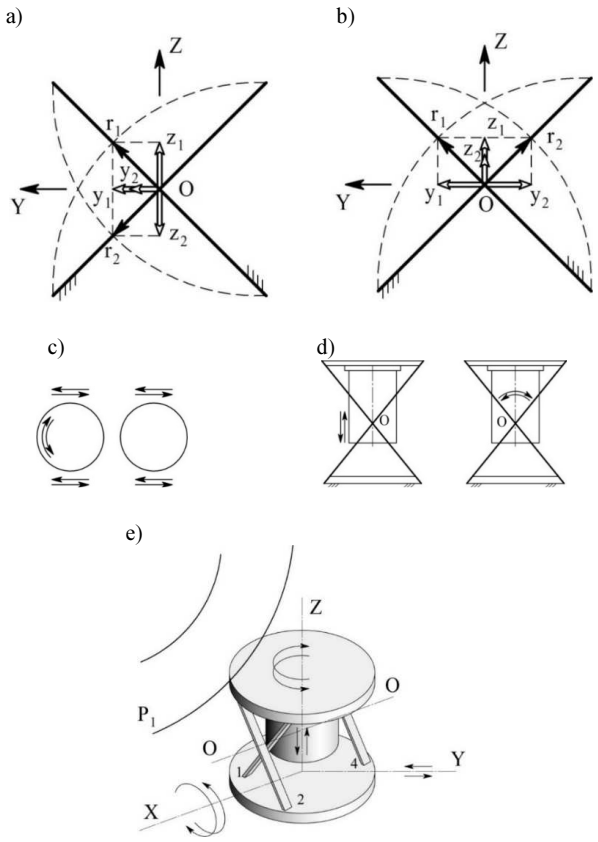

Fig. 3. A mechanism of elastic interaction of acoustic radiation with the device on an elastic suspension.

A number of issues of the plate dynamics, their physical structure and others under the influence of acoustic radiation is not completely understood yet. First of all, it refers to consideration of the boundary conditions when studying the plate with finite extent, which leads to an infinite system of equations describing the mechanical model.

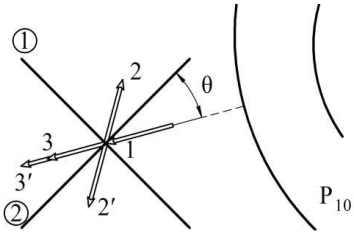

Fig. 4. A mechanism of pressure wave passing through an elastic suspension.

A characteristic feature of the geometry of boundary surfaces of elastic bodies is the presence of angular lines. Based on the formulation of boundary problems in the theory of elasticity in displacements (on the basis of the G. Lame's vector equation), there are three basic boundary problems, *i.e.* setting the vector of external forces on the body surface, setting the elastic

displacement vector on the body surface, and a mixed problem consisting of the fact that the forces are set on a part of the boundary surface, and a displacement vector is defined on the rest of the surface.

At present, two approaches have been developed, *i.e*. the method of homogeneous solutions, first applied by P. A. Schiff and V. A. Steklov, and the G. Lame's method of exact solutions. The first became a powerful means of asymptotic analysis of approximate shell theories. A prerequisite for the revival of the second one was the presence of a coherent theory of infinite systems and the emergence of PCs. Here, it is appropriate to mention the opening of asymptotic expression law by B. M. Koyalovich, which enabled establishing the lack of features in the expressions for stresses at the corner points and solving the first basic boundary problem. The analysis of flexural vibrations of finite plane bodies, *i.e.* elastic suspension plates, can also be carried out using the method described in the works of S. P. Tymoshenko. Its essence is to represent a mechanical disturbance and deflection of the plate as a double row by normal functions in the rectangular region. This method has the simplest mathematical interpretation, but still enables to investigate the dynamics of finite bodies deep enough. The dynamic properties of a flat infinite barrier in acoustic field have been studied in [1−7]. Sandwich-type constructions have been considered in [8−12]. The effect of sound waves on gimbals and other materials has been discussed in [13−24]. With regard to resonance manifestations in gimbals, they are usually focused on the impact of pedestal vibration and on the parametric resonance.

Such external perturbations as spatial waves has not been studied in terms of manifestations of gimbals' local peculiarities. We assume further that the elastic suspension plates have hinge fastenings at the ends, and thus the acoustic radiation energy will be absorbed completely by the oscillating plates, without affecting the adjacent structures.

3. Model of occurrence of plate resonant peculiarities

Transmission of acoustic waves through flat components in a form of infinite plates is thoroughly described by a simplified mathematical apparatus and significantly reduces analysis effort. This is quite enough for studying certain issues. Study of the dynamics of elastic interaction between flat barriers and an acoustic wave is limited to such models.

However, the approximate simulation modelling process has led to simplifications in which theoretical and experimental results lead to inconsistent findings. This primarily concerns the occurrence of local peculiarities.

The way out is to maximally approximate simulation models to real designs. In relation to the studied phenomena, it requires a transition from infinite to finite plates.

In this case flexural motion of finite flat bodies is advisable to be studied on the basis of external impact and plate flexure in a form of trigonometric series in the rectangular area. Let us consider a bi-dimensional problem. Let us suppose that the plate length is equal to a, its width to b, thickness to 2δ and is constant in the cross section. We also assume that the plate thickness is much less than other dimensions, *i.e.*: $2\delta << a$; $2\delta << b$.

The plate material would be absolutely elastic, homogeneous and isotropic. The length of flexural waves would be more than six times greater than the plate thickness, which would enable to use the equation of a thin plate.

Let us consider an acoustic field to be diffused.

In the light of those simplifications, it can be argued that the lateral sides of area element with a length of dy and width of dx remain in their motion parallel to xOz and yOz planes and perpendicular to the median plane (Fig. 5).

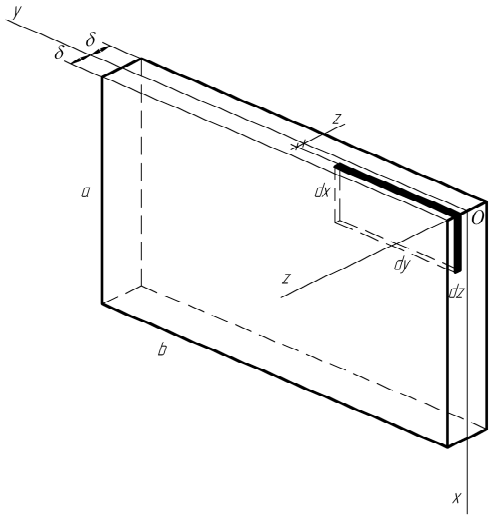

Fig. 5. A diagram of loading a spatial plate.

Whatever function of coordinates x, y would the plate flexion W be of, it can always be expressed by a two-fold series in the rectangular area in normal functions, *i.e.*:

$$W(x,y)=\sum_{m=1}^{\infty}\sum_{n=1}^{\infty}W_{mn}\sin\frac{m\pi x}{a}\sin\frac{n\pi y}{b}, \tag{1}$$

where: m = 1, 2, …, n = 1, 2, … are numbers of flexion half-waves along x and y axes, respectively; $W(x,y)$ is transmission of plate surface with coordinates x, y in the direction of z; $W_{mn}=W_{mn}(t)$ (Fig. 6).

It is easy to see that each term of series (1) meets the boundary conditions of:

$$\begin{aligned} &W\big|_{x=0}=0;\quad W\big|_{x=a}=0;\quad \left.\frac{\partial^2 W}{\partial x^2}\right|_{x=0}=0;\quad \left.\frac{\partial^2 W}{\partial x^2}\right|_{x=a}=0,\\ &W\big|_{y=0}=0;\quad W\big|_{y=b}=0;\quad \left.\frac{\partial^2 W}{\partial y^2}\right|_{y=0}=0;\quad \left.\frac{\partial^2 W}{\partial y^2}\right|_{y=b}=0. \end{aligned} \tag{2}$$

The relations (1) enable to calculate the maximum potential energy M_0, which accumulates in flexural plate deformation. For this purpose, it is sufficient to determine the maximum value of potential energy dM_0 of a surface element and then integrate the expression obtained in two ways:

$$\begin{aligned} M_0=\frac{1}{2}D\int_0^b\int_0^a\Bigg[&\left(\frac{\partial^2 W(x,y)}{\partial x^2}\right)^2+\left(\frac{\partial^2 W(x,y)}{\partial y^2}\right)^2+\\ &+2\sigma\frac{\partial^2 W(x,y)}{\partial x^2}\frac{\partial^2 W(x,y)}{\partial y^2}+2(1-\sigma)\left(\frac{\partial^2 W(x,y)}{\partial x\partial y}\right)\Bigg]dxdy, \end{aligned} \tag{3}$$

where: $D=8E\delta^3\left[12(1-\sigma)\right]^{-1}$ is cylindrical plate stiffness; E is the modulus of elasticity; σ is the Poisson's ratio.

The value of maximum kinetic energy T_0 at lateral oscillations of a plate is determined by the formula:

$$T_0 = \frac{1}{2}\omega^2 \mu \int_0^b \int_0^a W^2(x,y)dxdy, \tag{4}$$

where: μ is the specific weight; ω is a cyclical frequency.

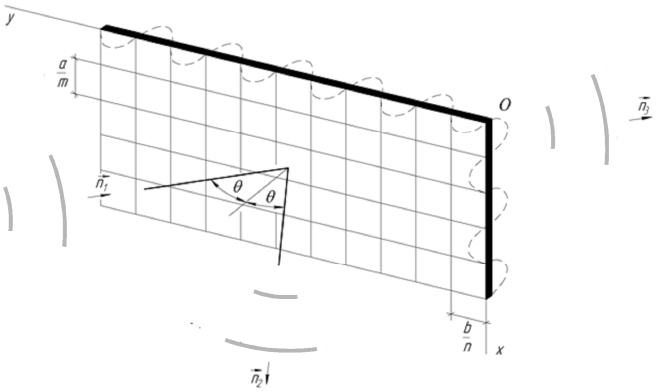

Fig. 6. Distribution of plate flexures: *m*, *n* are numbers of half-waves.

Let us apply the general equation of dynamics to build a differential equation of the plate in principal coordinates. This gives the following:

$$\mu W_{mn} + D\pi^4 \left(\frac{m^2}{a^2} + \frac{n^2}{b^2}\right) W_{mn} = Q_{m_1 n_1}, \tag{5}$$

where: $\pi^2 \left(D\mu^{-1}\right)^{\frac{1}{2}} \left(\frac{m^2}{a^2} + \frac{n^2}{b^2}\right) = \omega_{mn}$ is a natural oscillation frequency; $Q_{m_1 n_1}$ is a generalized force.

So, if an incident sound wave $P(x, y)$would be represented in a form of:

$$P(x,y) = \sum_{m=0}^{\infty} \sum_{n=0}^{\infty} P_{m_1 n_1} \sin \frac{m_1 \pi x}{a} \sin \frac{n_1 \pi y}{b}, \tag{6}$$

where: $P_{m_1 n_1}$ is a pressure amplitude of the appropriate form; m_1, n_1 are forms of sound pressure half-waves occurring both in length and width, then its virtual work will be calculated according to the formula:

$$\delta A = \int_0^b \int_0^a P_1(x,y,t)\delta W_{mn} \sin \frac{m_1 \pi x}{a} \sin \frac{n_1 \pi y}{b} dxdy. \tag{7}$$

Setting for specificity:

$$P_1(x,y,t) = P_{10} \exp i\left\{\omega t - k\left[x \sin\theta + (y-\delta)\cos\theta\right] + \frac{\pi}{2}\right\}, \tag{8}$$

where: P_{10} is a pressure amplitude; k is a wave number, we obtain:

$$Q_{m_1 n_1} = P_{10} \exp i\left(\omega t - k\delta\cos\theta + \frac{\pi}{2}\right) \exp i\left[k\left(b\cos\theta - a\sin\theta\right)\right] \left\{\left[S_1 m_1 \pi a^{-1} \exp i\left(ka\sin\theta\right) - \right.\right.$$
$$\left.\left. - S_2 n_1 \pi b^{-1} \exp i\left(kb\cos\theta\right) - S_1 S_2\right] \left\{\left(k\cos\theta\right)^2 + \left(n_1 \pi b^{-1}\right)^2 \left[\left(k\sin\theta\right)^2 + \left(m_1 \pi a^{-1}\right)^2\right]\right\}, \tag{9}$$

from the expression (7).

When $0 < m_1 << 1$, $0 < n_1 << 1$, which corresponds to loading evenly distributed over the plate area, the formula (9) would be converted to the form:

$$Q_{m_1 n_1} = P_{10} ab \left(m_1 n_1\right)^{-1} \left(1 - \cos m_1 \pi\right)\left(1 - \cos n_1 \pi\right). \tag{10}$$

The generalized force Q will be zero for even values m_1 and n_1, *i.e.*:

$$Q_{m_1 n_1} = 0 . \tag{11}$$

And vice versa, for odd values:

$$Q_{m_1 n_1} = 4P_{10}ab\left(m_1 n_1 \pi^2\right)^{-1} . \tag{12}$$

By calculating the maximum work A_0 of an incident sound pressure wave, according to the formula:

$$A_0 = \int_0^b \int_0^a P(x,y)W(x,y)dxdy , \tag{13}$$

let us establish the law of plate flexural vibrations on the basis of extreme properties of its bending:

$$\frac{\partial}{\partial W_{mn}}\left(T_0 - M_0 + A_0\right) = 0 . \tag{14}$$

If consideration of energy dissipation due to the internal friction is required, it would be enough to consider the work of these forces in the expression (14), *i.e.*:

$$\frac{\partial}{\partial W_{mn}}\left(T_0 - M_0 + A_0 - R_0\right) = 0 , \tag{15}$$

where:

$$R_0 = \frac{\chi}{2}\int_0^b \int_0^a W^2(x,y)dxdy = \frac{1}{8}\mu\eta ab\omega^2 \sum_{m=1}^{\infty}\sum_{n=1}^{\infty} W_{mn}^2 , \tag{16}$$

$\chi = \eta\mu\omega_{mn}^2$ is an internal friction coefficient; η is a coefficient of losses.

Let us suppose that $m_1 = m$, $n_1 = n$.

These conditions imply the coincidence of a number of acoustic radiation half-waves and plate vibration generated in two directions: along axis x ($m_1 = m$) and along axis y ($n_1 = n$).

Substituting the relation (1), (8) in the expressions (3), (4) and (13), we obtain the following:

$$\begin{aligned} M_0 &= \frac{1}{8}Bab\pi^4 \sum_{m=1}^{\infty}\sum_{n=1}^{\infty}\left(\frac{m^2}{a^2} + \frac{n^2}{b^2}\right)W_{mn}^2(x,y), \\ T_0 &= \frac{1}{8}\mu ab\omega^2 \sum_{m=1}^{\infty}\sum_{n=1}^{\infty} W_{mn}^2(x,y), \\ A_0 &= \frac{1}{4}ab\sum_{m=1}^{\infty}\sum_{n=1}^{\infty} P_{mn}W_{mn}(x,y). \end{aligned} \tag{17}$$

On the basis of the extrenality condition (15), the expressions (17) give an opportunity to find out the value of bend for each pair of indices m and n:

$$W_{mn}(x,y) = \frac{P_{mn}}{\mu\left(\omega_{mn}^2 - \omega^2\right)}, \tag{18}$$

where ω_{mn} is a natural frequency calculated from the above formula.

It is clear that under the occurrence of $\omega = \omega_{mn}$, the plate flexure constantly grows and it becomes acoustically *transparent.*

Substituting the value of generalized force Q_{mn} (19) in the differential equation of motion (5), the law of plate flexural vibrations can be established on the mn form at the continuous action of sound radiation in a time interval [0, t]. It contains its natural and forced vibrations, *i.e.*:

$$W_{mn}(x,y,t) = \omega_{mn}^{-1}\int_0^t Q_{mn}\mu^{-1}\sin\omega_{mn}(t-t_1)dt_1 =$$
$$= P_{10}\exp i\left\{\omega t + k\left[(b-\delta)\cos\theta - a\sin\theta\right] + \frac{\pi}{2} + tg\varphi(t)\right\}\times \tag{19}$$
$$\times\left\{\left[S_1 m\pi a^{-1}\exp i(ka\sin\theta) - S_2 n\pi b^{-1}\exp i(kb\cos\theta) - S_1 S_2\right] + mn\pi^2(ab)^{-1}\right\}\times$$
$$\times\left\{\mu\left(\omega_{mn}^2 - \omega^2\right)\left[(k\cos\theta)^2 + (n\pi b^{-1})^2\right]\left[(k\sin\theta)^2 + (m\pi a^{-1})^2\right]\right\}^{-1}.$$

Finally, considering the relation (19) we obtain:

$$W(x,y,t) = \sum_{m=1}^{\infty}\sum_{n=1}^{\infty} W_{mn}(x,y,t)\sin\frac{m\pi x}{a}\sin\frac{n\pi y}{b} =$$
$$= P_{10}\sum_{m=1}^{\infty}\sum_{n=1}^{\infty}\rho(t)\left\{\mu\left(\omega_{mn}^2 - \omega^2\right)\left[(k\cos\theta)^2 + (n\pi b^{-1})^2\right]\left[(k\sin\theta)^2 + (m\pi a^{-1})^2\right]\right\}^{-1}\times$$
$$\times\exp i\left\{\omega t + k\left[(b-\delta)\cos\theta - a\sin\theta\right] + \frac{\pi}{2} + tg\varphi(t)\right\}\times \tag{20}$$
$$\times\left\{\left[S_1 m\pi a^{-1}\exp i(ka\sin\theta) - S_2 n\pi b^{-1}\exp i(kb\cos\theta) - S_1 S_2\right] + mn\pi^2(ab)^{-1}\right\}\times$$
$$\times\sin\frac{m\pi x}{a}\sin\frac{n\pi y}{b},$$

from the expression (1),where: $\rho(t) = \left[(\cos\omega t - \cos\omega_{mn}t)^2 + (\sin\omega t - \omega\omega_{mn}^{-1}\sin\omega_{mn}t)^2\right]^{\frac{1}{2}}$;
$tg\varphi(t) = (\sin\omega t - \omega\omega_{mn}^{-1}\sin\omega_{mn}t)(\cos\omega t - \cos\omega_{mn}t)^{-1}$.

The same is for the case of acoustic loading uniformly distributed over the plate area. For this purpose, it is enough to substitute the relations (12) in (5). We obtain:

$$W_{mn}(x,y,t) = 16gP_{10}\left(\mu mn\pi^2\omega_{mn}^2\right)^{-1}(1-\cos\omega_{mn}t). \tag{21}$$

Now the pattern of plate flexural motion can be established:

$$W(x,y,t) = 16gP_{10}\left(\mu\pi^2\right)^{-1}\sum_{m=1}^{\infty}\sum_{n=1}^{\infty}\left(mn\omega_{mn}^2\right)^{-1}(1-\cos\omega_{mn}t)\sin\frac{m\pi x}{a}\sin\frac{n\pi y}{b}, \tag{22}$$

where m and n are odd numbers.

For a finite plate, the flexural motion can be represented as the superposition of forced vibrations of an infinite plate and natural vibrations that occur in the plate given its size.

If a plate impedance on the *mn* form is:

$$Z_{mn} = P_{mn}V_{mn}^{-1} = i\mu\omega\left[(c_3 c^{-1}\sin\theta)^4 - (\omega^{-1}\omega_{mn})^2\right], \tag{23}$$

then it becomes clear that – even fulfilling the wave coincidence condition $c_3 = c\sin^{-1}\theta$, but if there is no equality of frequencies ω_{mn} of finite plate natural vibrations and frequencies ω of infinite plate forced vibrations – the flexures would have a fixed value. The plate would be acoustically *transparent*, *i.e.* the equality $Z_{mn} = 0$ would occur only if both conditions are fulfilled:

$$\begin{aligned} c_3 &= c\sin^{-1}\theta, \\ \omega &= \omega_{mn}. \end{aligned} \tag{24}$$

4. Discussion of results of plate flexures by vibration forms

Let us perform a numerical analysis of lower vibration forms, having assumed the following parameters for the sake of clarity: $2\delta = 2 \cdot 10^{-3}\, m,\ \ \sigma = 0,3,\ \ E = 710\ Nm^{-2}.\ \ \theta = \frac{\pi}{4} rad,\ \ \omega = 100\ s^{-1},$ $a = 0,1\ m,\ \ b = 0,2\ m.$ The quantitative analysis shows that the maximum deflection of an elastic suspension plate is observed at the first (lowest) waveform, that is when $m_1 = m_k = 1,\ \ n_1 = n_k = 1.$ Higher waveforms have a more complex structure of the bending motion. For example, upon $m_1 = m_k = 1\ ,\ \ n_1 = n_k = 2,$ each of the plates has, unlike the first form, two local extrema of opposite polarity, while upon $m_1 = m_k = 1\ ,\ \ n_1 = n_k = 3$ they have three extrema. The higher the form number, the more complex the bending movement of the suspension plates. Obviously, the number of extrema is determined by the product $m_k \cdot n_k$.

The analysis shows that upon an odd n, the bend magnitude is much larger in absolute terms than upon an even n. Thus, these forms will contribute to a more intense sonic energy pumping. The numerical values of maximum plate flexures for the first five forms of vibration are shown in Table 1. The values of natural frequencies ω_{mn} of vibration $m_k n_k$ – forms are shown in Table 2. Here, P_{10} is a normalizing factor.

The numerical analysis proves that the maximum plate flexures are on the first – the lowest – form, *i.e.* when $m_1 = m = 1;\ n_1 = n = 1.$

Thus, the most favourable for the device is a combination of 1 waveforms of one plate with even waveforms of the other one, *i.e.* 2, 4, 6, *etc*. (Fig. 7a). In this case, as can be seen, the movement of the device output axis in the direction of Y axis is only due to fluctuations of the first plate r_1, and there is no movement towards Z axis. If there is a combination of the first waveform of one plate and odd forms (1, 3, 5, 7, *etc*.) of the other, there is the most complex motion of the suspension axis, both in the direction of Y axis and in the direction of Z axis (Fig. 7b). There is both translational and angular acoustic suspension vibration.

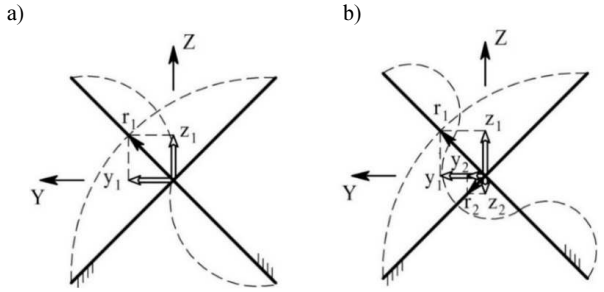

Fig. 7. The effect of a plate waveform on the movement of the device output axis.

Table 1. The maximum plate flexures.

$m = m_1$	$n = n_1$	W_{max}/P_{10}, m
1	1	15
1	2	$12*10^{-4}$
1	3	4,8
1	4	$5,9*10^{-4}$
1	5	2,9
2	2	$11,8*10^{-4}$
3	3	4,8
4	4	$5,6*10^{-4}$
5	5	2,9

Table 2. The values of natural plate frequencies.

$m = m_1$	$n = n_1$	ω_{mn}, s^{-1}	$m = m_1$	$n = n_1$	ω_{mn}, s^{-1}
1	1	0,376	4	1	4,888
	2	0,602		2	5,114
	3	0,978		3	5,490
	4	1,504		4	6,016
	5	2,181		5	6,693
2	1	1,278	5	1	7,595
	2	1,504		2	7,821
	3	1,880		3	8,197
	4	2,406		4	8,723
	5	3,083		5	9,340
3	1	2, 782			
	2	3,008			
	3	3,384			
	4	3,910			
	5	4,587			

Thus, the elastic interaction of a gyroscope suspension with acoustic radiation perturbs the device motion and, consequently, leads to the emergence of measurement errors. The most dangerous are odd vibration forms, which transmit maximum sound energy

5. Conclusions

The research show that, regarding the operating conditions, the base element of gimbals and its components goes into the category of impedance structures interacting elastically with penetrating acoustic radiation. Therefore, the on-board equipment needs to be placed in acoustic comfort.

Methods for solving this task depend on what is more important - high positioning accuracy or weight of the missile/aircraft.

Finally, special attention should be paid to the risk of resonance phenomena, in particular the spatial-frequency resonance. Ways to solve this problem have not yet been sufficiently developed, because of the spatial nature of N-wave and penetrating radiation, unlike force and kinematic impacts penetrating into devices only through supports.

Acknowledgements

The Industrial Research Institute for Automation and Measurements is kindly acknowledged for covering the costs of publishing of the paper.

References

[1] Beshenkov, S.N. (1974). *Study of acoustic properties of sandwich constructions.* Acoustic Magazine, 20 (2), 276–281.

[2] Madeira, J.F.A., Araújo, A.L., Mota Soares, C.M., Mota Soares, C.A., Ferreira, A.J.M. (2015). *Multiobjective design of viscoelastic laminated composite sandwich panels. Composites Part B: Engineering*, 77(1), 391–401.

[3] Wang, T., Li, S., Nutt, S.R. (2009). Optimal design of acoustical sandwich panels with a genetic algorithm. *Applied Acoustics*, 70(3), 416–425.

[4] Chronopoulos, D., Collet, M., Ichchou, M., Antoniadis, I. (2015).Wave based design optimisation of composite structures operating in dynamic environments. *COMPDYN 2015 – 5th ECCOMAS Thematic Conference on Computational Methods in Structural Dynamics and Earthquake Engineering*, 4390–4408.

[5] Bogolepov, I.I. (1986). Industrial soundproofing. *Monograph. L. Sudostroenie*, 386.

[6] Brekhovskih, I.M. (1973). Waves in layered structures. *Monograph. M. Nauka*, 344.

[7] Valeev, K.G. (1970). Definition of stress state of flat panels in the acoustic field of the exhaust stream. *Adventure of Mechanic*, VI(4), 30–43.

[8] Goloskokov, E.G. (1980). Elastic and acoustic problems of sandwich construction dynamics. *Monograph. Kharkiv. Vyshcha shkola*, 189.

[9] Kanibolotskiy, M.A. (1980). Optimal design of layered structures. *Monograph. Novosibirsk. Nauka. Sib. Department*, 176.

[10] Xu, F., Wang, W., Shao, X., Liu, X., Liang, Y. (2015). Optimization of surface acoustic wave-based rate sensors. *Sensors*, 15(10,12), 25761–25773.

[11] Hamdaoui, M., Robin, G., Jrad, M., Daya, E.M. (2014). Optimal design of frequency dependent three-layered rectangular composite beams for low mass and high damping. *Composite Structures*, 120, 174–182.

[12] Karachun, V., Mel'nick, V., Korobiichuk, I., Nowicki, M., Szewczyk, R., Kobzar, S. (2016). The Additional Error of Inertial Sensor Induced by Hypersonic Flight Condition. *Sensors*, 16(3).

[13] Karachun, V.V. (2012). Influence of Diffraction Effects on the Inertial Sensorg of a Gyroscopically Stabilized Platform: Three-Dimansional Problem. *International Applied Mechanics*, 48(4), 458–464.

[14] Karachun, V.V. (2014). Ware coincidence and errors of floating gyroscope at the resonance Level. News of Science and Education, *Technical Science, Mathematics. Science and Education Ltd*, 31(21), 56–62.

[15] Karachun, V.V. (1989). Vibration of a plate under an acoustic load. *Engineering, Technology Science, PA*, 20(37), 391–394.

[16] Mostafapour, A., Ghareaghaji, M., Davoodi, S., Ebrahimpour, A. (2016). Theoretical analysis of plate vibration due to acoustic signals. *Applied Acoustics*, 103, 82–89.

[17] Geng, Q., Li, Y. (2012). Analysis of dynamic and acoustic radiation characters for a flat plate under thermal environments. *International Journal of Applied Mechanics*, 4(3).

[18] Alzahabi, B., Almic, E. (2011). Sound radiation of cylindrical shells. *International Journal of Multiphysics*, 5(2), 173–185.

[19] Korobiichuk, I. (2016). Mathematical model of precision sensor for an automatic weapons stabilizer system. *Measurement*, 89, 151–158.

[20] Lee, S.W., Rhim, J.W., Park, S.W., Yang, S.S. (2007). A novel micro rate sensor using a surface-acoustic-wave (SAW) delay-line oscillator. *Proc. of IEEE Sensors*, 1156–1159.

[21] Korobiichuk, I., Nowicki, M., Szewczyk, R. (2015). Design of the novel double-ring dynamical gravimeter. *Journal of Automation, Mobile Robotics and Intelligent Systems*, 9(3), 47–52.

[22] Mehta, A., Jose, K.A., Varadan, V.K. (2002). Numerical simulation of a surface acoustic wave (SAW) gyroscope using HP EEsof. *Proc. of SPIE. The International Society for Optical Engineering*. 4700, 169–177.

[23] Korobiichuk, I., Koval, A., Nowicki, M., Szewczyk, R. (2016). Investigation of the Effect of Gravity Anomalies on the Precession Motion of Single Gyroscope Gravimeter. *Solid State Phenomena*, 251, 139–145.

[24] Creagh, M.A., Beasley, P., Dimitrijevic, I., Brown, M., Tirtey, S. (2012). A Kalman-filter based Inertial navigation system processor for the SCRAMSPACE 1 hypersonic flight experiment. *18th AIAA/3AF International Space Planes and Hypersonic Systems and Technologies Conference 2012*, Tours, France.